Smart Mater. Struct. **22** (2013) 065004 (8pp) doi:10.1088/0964-1726/22/6/065004

Metamaterial-inspired structures and concepts for elastoacoustic wave energy harvesting

M Carrara[1], M R Cacan[2], J Toussaint[2], M J Leamy[2], M Ruzzene[1,2] and A Erturk[2]

[1] D Guggenheim School of Aerospace Engineering, Georgia Institute of Technology, Atlanta, GA 30332, USA
[2] G W Woodruff School of Mechanical Engineering, Georgia Institute of Technology, Atlanta, GA 30332, USA

Received 6 November 2012, in final form 8 March 2013
Published 26 April 2013
Online at stacks.iop.org/SMS/22/065004

Abstract
Enhancement of structure-borne wave energy harvesting is investigated by exploiting metamaterial-based and metamaterial-inspired electroelastic systems. The concepts of wave focusing, localization, and funneling are leveraged to establish novel metamaterial energy harvester (MEH) configurations. The MEH systems transform the incoming structure-borne wave energy into electrical energy by coupling the metamaterial and electroelastic domains. The energy harvesting component of the work employs piezoelectric transduction due to the high power density and ease of application offered by piezoelectric materials. Therefore, in all MEH configurations studied in this work, the metamaterial system is combined with piezoelectric energy harvesting for enhanced electricity generation from waves propagating in elastic structures. Experiments are conducted to validate the dramatic performance enhancement in MEH systems as compared to using the same volume of piezoelectric patch in the absence of the metamaterial component. It is shown that MEH systems can be used for both broadband and tuned wave energy harvesting. The MEH concepts covered in this paper are (1) wave focusing using a metamaterial-inspired parabolic acoustic mirror (for broadband energy harvesting), (2) energy localization using an imperfection in a 2D lattice structure (for tuned energy harvesting), and (3) wave guiding using an acoustic funnel (for narrow-to-broadband energy harvesting). It is shown that MEH systems can boost the harvested power by more than an order of magnitude.

(Some figures may appear in colour only in the online journal)

1. Introduction

The transformation of vibrations into electricity has been heavily researched for powering small electronic components employed in various engineering systems, ranging from unmanned aerial vehicles [1, 2] to bridges [3, 4]. The main research motivation for this field derives from the reduced power requirement of small electronic components, such as wireless sensor networks used in passive and active monitoring applications. The ultimate goal is to power such small electronic devices by using vibrational energy available in their environment such that the need for and costs of battery replacement and disposal can be minimized. Among the basic transduction mechanisms, piezoelectric transduction [5–9] offers the highest power density and relative ease of application [10] for converting kinetic/strain energy into electricity. Although the harvesting of direct vibrational energy is well studied, limited effort has been devoted to exploiting the energy of waves propagating in structures and fluids. A few research groups have addressed this area through the use of Helmholtz resonators [11, 12], sonic crystals [13, 14], and polarization-patterned piezoelectric solids [15]. Others have investigated

aeroelastic and hydroelastic phenomena for flow energy harvesting [16–26].

Various heterogeneous structures and materials feature geometric, micro-structural and/or material properties that vary periodically in space. Periodic metamaterials can be designed to exhibit non-traditional physical behaviors such as negative stiffness, mass, and Poisson's ratio. In order to exploit periodic metamaterials for energy harvesting, the present paper explores their unique ability to guide the propagation of elastic waves and their ability to focus their energy [27–29]. These abilities have been exploited for the design of innovative actuators and sensors, and elements of logic circuitry based on the propagation of elastic waves [30, 31]. Wave guiding and focusing can be achieved through operation within a bandgap frequency range, and the introduction of controlled levels of disorder or engineered defects. Property modulations and engineered anisotropy in heterogeneous media can also produce negative refractive indices, which lead to super-lensing or super-focusing characteristics [32]. Numerous potential implications of this mechanical wave guiding technology exist, including active sensing of structural integrity, smart sensing of the environment for the purposes of vehicle steering or guidance, and dissipation of high-frequency modes of vibration, among others. Of particular interest in this paper is the investigation of how guided waves can assist in steering energy towards sinks that either absorb energy or perform its transduction.

Innovative metamaterial energy harvester (MEH) systems capable of enhanced harvesting of structure-borne elastoacoustic waves are introduced herein. In particular, three concepts are explored in conjunction with piezoelectric power generation: (1) focusing using a parabolic acoustic mirror, (2) localization using a 2D lattice structure with an imperfection, and (3) guiding and channeling using an acoustic funnel. The first and the third concepts are shown to be capable of *broadband* wave energy harvesting, while the second is introduced for *tuned* wave energy harvesting. Experimental verifications are presented in order to compare the harvested energy in the presence and absence of the proposed focusing devices.

2. Wave focusing using a parabolic acoustic mirror

2.1. Concept of plane wave focusing and numerical simulations

The elliptical acoustic mirror (EAM) described in [33] was proved to be a very effective means of focusing propagating waves, but it has the inherent drawback of needing the *point* source location to be known *a priori*, which can be impractical for real-life scenarios. In order to overcome this limitation and incorporate harvesting of *plane* waves originating from an unknown source, the first concept introduced is a parabolic acoustic mirror (PAM). In this case the scatterers consist of cylindrical stubs mounted on the surface of a plate, which supports the propagation of Lamb waves. The goal is to enable a configuration that can capture and focus the incoming plane wave energy in space (at the focus of the parabola) where the harvester is located. The arrangement of the stubs is selected with the goal of achieving broadband focusing capabilities. The parabolic arrangement of stubs ensures focusing of *plane waves*, while the spacing of the stubs along the parabola is smaller or on the order of the wavelength of the considered Lamb wave mode (namely, A_0 mode) so that the array behaves approximately as a perfect acoustic mirror [33].

The focusing capabilities of the PAM are investigated first numerically through simulations which predict the interaction of a plane wave with the parabolic mirror. A multiple-scattering problem is formulated using a Green's function formalism [35], whereby the thin plate is an infinite medium, and each stub acts as a point scatterer. The plane wave generation is achieved numerically by considering the constructive interaction of point sources laid out along a linear array path [34].

The out-of-plane displacement of the plate at a generic position $\boldsymbol{x}$ produced by a distribution of N_s point sources with constant intensity A is given by [35]

$$u(\boldsymbol{x}, \omega) = A\, g_0(\omega) \sum_{n=1}^{N_s} \mathcal{G}(\boldsymbol{x}, \boldsymbol{x}_n, \omega) \tag{1}$$

where $g_0(\omega)$ denotes the amplitude of the excitation at frequency ω, while $\mathcal{G}(x, x_n, \omega)$ denotes the Green's function defining the response to a unit source at $\boldsymbol{x}_n$ and is approximated as

$$\mathcal{G}(\boldsymbol{x}, \boldsymbol{x}_n, \omega) = \mathrm{j}\pi^2 H_0^{(1)}(\kappa(\omega) R_n). \tag{2}$$

Here, $H_0^{(1)}$ is the Hankel function of the first kind and order 0, and $R_n = |\boldsymbol{x} - \boldsymbol{x}_n|$ is the distance between the generic location $\boldsymbol{x}$ and the nth source. Dispersion is taken into account in the definition of the wavenumber $\kappa = \kappa(\omega)$ which matches the dispersion relations for the considered mode propagating in the isotropic thin plate.

Scattering events are modeled as additional sources providing an excitation proportional in amplitude to that of the incoming wavefield. The out-of-plane displacement field is then given by [35]

$$u(\boldsymbol{x}, \omega) = u^*(\boldsymbol{x}, \omega) + \sum_{m=1}^{M} u^*(\boldsymbol{x}_m, \omega) \tau_m \mathcal{G}(\boldsymbol{x}, \boldsymbol{x}_m, \omega) \tag{3}$$

where τ_m is the scattering coefficient (which is assumed to be unity for the quantitative simulation of the problem), M is the total number of scatterers defining the mirror, $u^*(\boldsymbol{x}, \omega)$ is the wavefield at $\boldsymbol{x}$ resulting from summation of the applied excitation and of scattering events accounted for through a repeated application of the previous expressions.

The simulation considers the configuration of figure 1(a), where a 1 mm thick aluminum plate is excited by a linear array of sources using a 4-cycles tone burst of central frequency of 50 kHz. For simplicity, the source amplitude, and the scattering coefficient, are set to unity, and one single interaction between scatterers is assumed. Figure 1(b) displays the spatial distribution of the RMS displacement field and illustrates the focusing of the incoming plane wave energy at the location of the energy harvester.

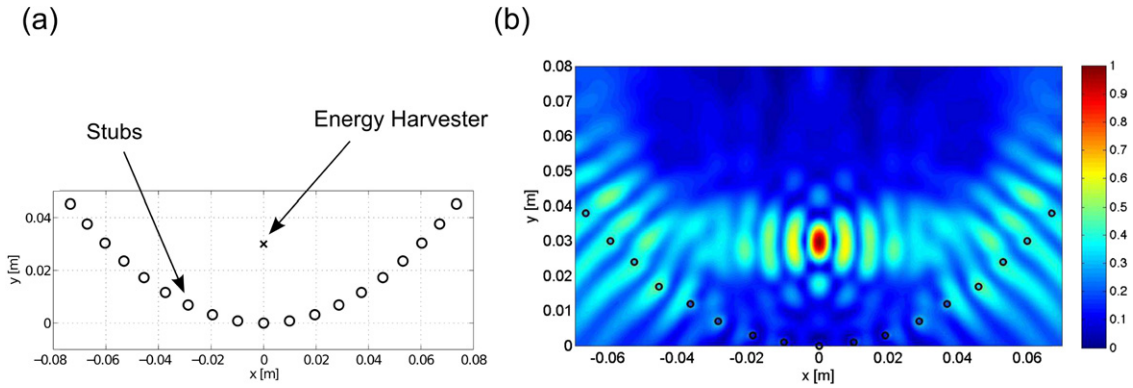

Figure 1. (a) Schematic representation of the PAM configuration showing the location of the piezoelectric energy harvester; (b) detail of the simulated RMS displacement distribution exhibiting focusing of the wave energy at the location of the energy harvester.

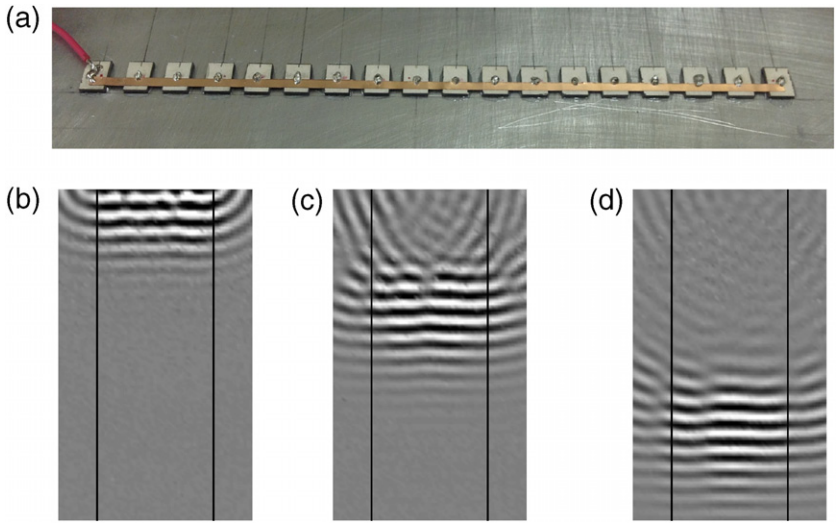

Figure 2. Experimental plane wave generation: (a) linear PZT source array, (b)–(d) snapshots of the wavefield propagating from the array (bounded by vertical black lines).

2.2. Experimental setup, plane wave generation and focusing

In order to investigate the harvesting performance of the PAM concept, a practical means of generating a directional plane wave is addressed first using a linear array of rectangular PZT patches, as depicted in figure 2(a). All elements of the array are excited *in phase* with a 4-cycles windowed tone burst at a central frequency of 50 kHz. Full wavefield snapshots are presented in figures 2(b)–(d). From the former it can be visually inferred that a well-shaped plane wave region exists within the boundaries of the array itself. Furthermore, the latter confirms that the desired strong directionality is achieved.

The experimental PAM arrangement is depicted in figure 3(a) while the reference configuration (without the PAM) used for performance comparison in the energy harvesting tests is shown in figure 3(b). The source is provided by the previously shown linear PZT array, while the harvester is a piezoelectric disk of 7 mm diameter and 0.2 mm thickness. All the PZT elements (STEMiNC Corp.) are bonded to a 1 mm thick aluminum plate. The source array is excited by sinusoidal 4 cycle tone burst at selected frequencies, provided by a function generator (Agilent 33220A) through a voltage amplifier (Trek Model PZD350). The resulting wave propagation field is measured by a scanning laser vibrometer (Polytec PSV-400). Wavefield images and RMS distributions are obtained by recording the plate response over a grid of points that cover the PAM and free harvester region.

The experimental RMS distribution of the velocity field for excitation at 50 kHz presented in figure 4(a) shows very good agreement with the simulations (figure 1(b)), and demonstrates the focusing effect of the PAM at the location of the harvester. It is worth noting that for the experimental case the energy is more spread in the vicinity of the focus region with respect to the numerical case. This is probably due to small misalignments between the parabola axis and the wavefront.

Next, the broadband focusing characteristics of the PAM are investigated by performing experiments at various frequencies in the 30–100 kHz range. At each frequency, the response of the plate is measured along the centerline of the PAM ($x = 0$ mm in figure 3). The results are summarized

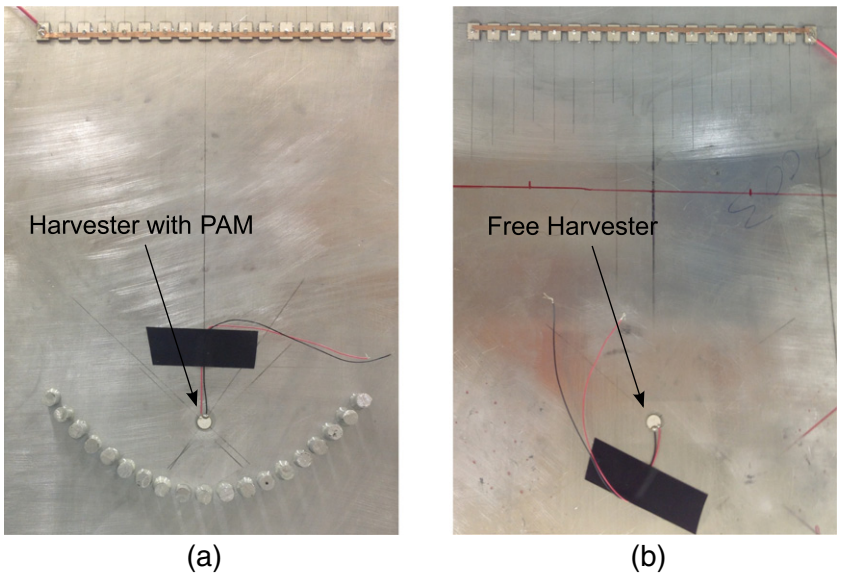

Figure 3. Experimental structure-borne wave energy harvesting configurations: (a) energy harvester located at the focus of the PAM configuration; (b) free energy harvester configuration in the absence of the PAM for comparison of the generated electrical power for the same wave excitation and the same distance from the source array.

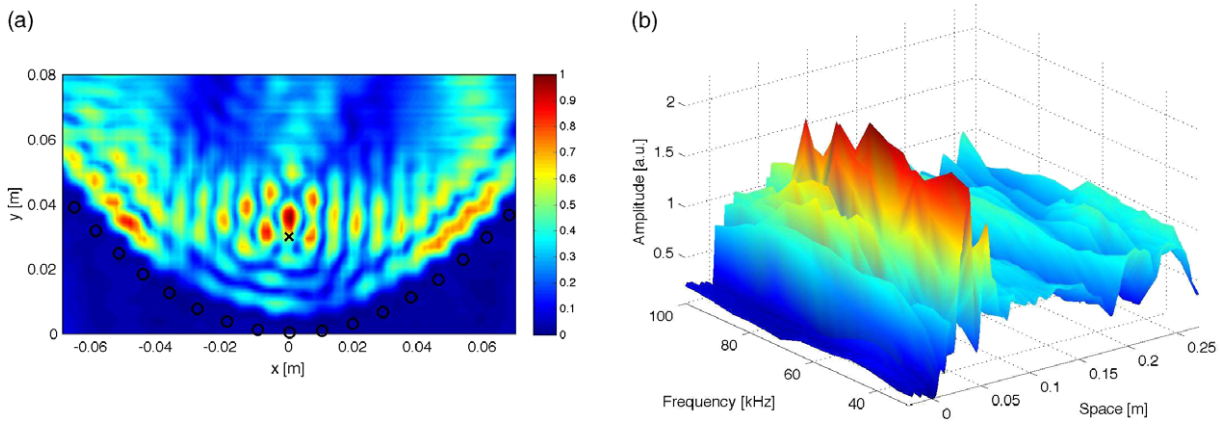

Figure 4. (a) Experimentally measured RMS velocity field for excitation at 50 kHz (the source region is excluded) for the PAM configuration shows wave focusing at the location of the energy harvester; (b) normalized experimental RMS velocity field along the major axis ($x = 0$ mm) of the semi-ellipse for the frequency range 30–100 kHz.

in figure 4(b), which shows the variation of the normalized wave amplitude along the centerline as a function of the excitation frequency. The results clearly illustrate how the sources (located at $y = 230$ mm) create a velocity field that is amplified by the acoustic mirror to yield a peak at the focal point of the parabolic mirror (located at $y = 30$ mm). The amplitude of this peak varies with frequency, and reaches its maximum values around 50 kHz. Above this frequency, a general decaying trend for the amplitude at the focus is observed, which may be explained by the decreasing wavelength of the selected mode with frequency. This directly leads to a reduced effectiveness of the PAM (which becomes very evident starting from 80 kHz) due to the effect of the spacing of the stubs (in this case 10 mm along the parabolic path), which becomes higher than the A_0 wavelength at frequencies higher than 50 kHz.

2.3. Energy harvesting performance

The performance of the PAM-based wave energy harvesting concept (figure 3(a)) is investigated experimentally and compared to that of a *free* wave energy harvester (figure 3(b)). In order to characterize and compare the electrical power outputs for the configurations with and without the PAM, sets of resistor sweeps are performed. The voltage input is taken to be a continuous harmonic and the frequency is varied from 30 to 80 kHz to further test the broadband characteristics of the PAM configuration. Figure 6(a) shows the time history of the voltage output across a resistive electrical load of 1.3 kΩ at 55 kHz. This electrical load is around the optimal electrical estimated load, based on the relation $R = 1/\omega C$, where the excitation radial frequency and the piezoelectric capacitance are $\omega = 110k\pi$ rad s^{-1} and $C = 2.2$ nF, respectively. The voltage output is substantially increased in the PAM-based

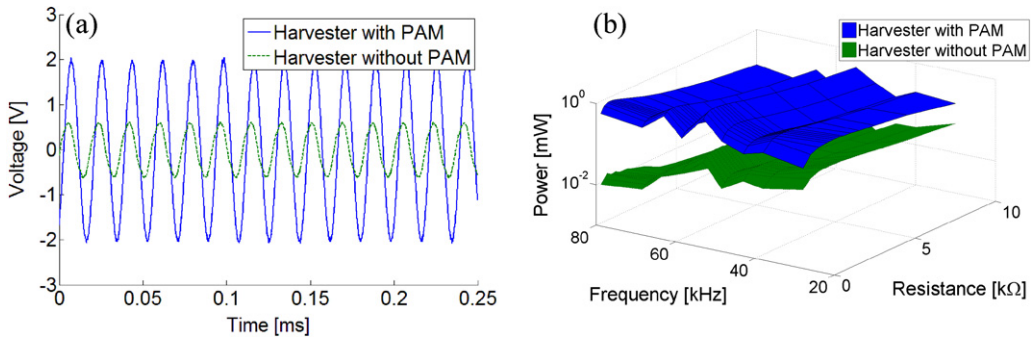

Figure 5. Comparison of piezoelectric energy harvesters with and without the PAM configuration: (a) voltage output histories at 55 kHz for 1.3 kΩ exhibiting the advantage of the PAM-based energy harvester; (b) power versus load resistance and frequency surfaces for the frequency range 30–80 kHz covering the region of the optimal electrical load at each frequency.

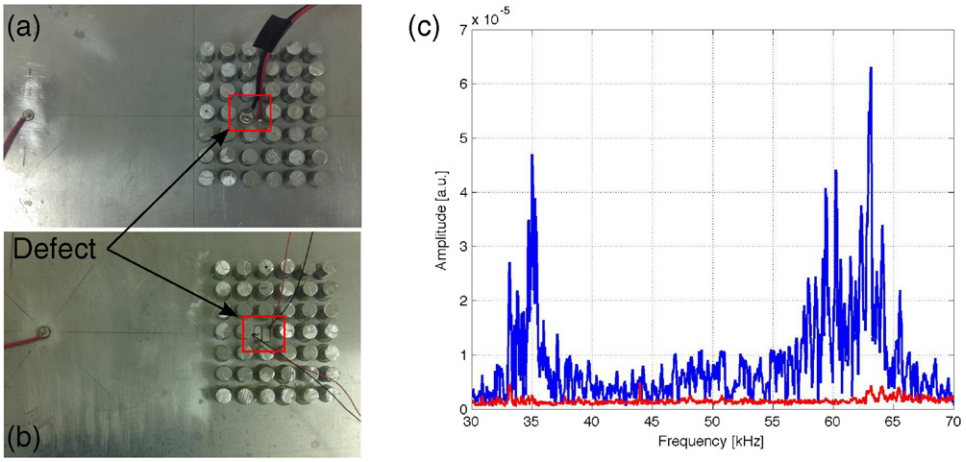

Figure 6. 2D lattice structure made of aluminum stubs with an imperfection where (a) a circular energy harvester and (b) two rectangular harvesters are located; (c) frequency response function comparison for the circular harvester case. Blue line: point inside the defect. Red line: point belonging to the stubbed region.

harvester as compared to the free energy harvester without the PAM.

Results of the energy harvesting capabilities of the PAM-based configuration, shown in figure 5(b), exhibit substantially enhanced power generation performance over a wide range of excitation frequencies. The maximum power generated by the PAM-based energy harvester occurs at 55 kHz and 1.3 kΩ with 1.51 mW, whereas the free harvester showed a maximum at 55 kHz and 1.7 kΩ producing 145 μW of power. Across all resistance and frequency levels, the system shows an average of 1800% increase over the free harvester case.

3. Wave localization using a 2D lattice with an imperfection

3.1. Concept of wave localization and experimental setup

The second concept introduced herein is proposed for *tuned* wave energy harvesting. This MEH system features a periodic array with an internal defect that is realized by breaking the lattice periodicity by the removal of one internal stub, as shown in figures 6(a)–(b). The localization of the energy at the imperfection can be exploited for tuned energy harvesting purposes. The fundamental idea is to create a match between the defect resonance frequency and the excitation frequency. Due to the metamaterial nature of the lattice, the concept can be extended to match the frequency content of specific applications, and thus it can be considered as completely tailorable.

3.2. Frequency response of the defect

Experimental tests are performed in order to evaluate the feasibility of the concept. The frequency response functions (output/input voltage recorded from the SLDV) for two points inside and outside the defect of the stubbed region are presented in figure 6(c). Two peaks are highlighted for the point inside the defect, at 35 and 63 kHz, respectively. Taking advantage of the scanning capability of the vibrometer, full wave propagation field data of the slab are recorded for harmonic excitation at the above-cited frequencies. The normalized RMS results presented in figures 7(a)–(b) clearly show that the first frequency corresponds to the first mode of the defect, while the second frequency excites the second mode. It is worth mentioning that these are indeed the

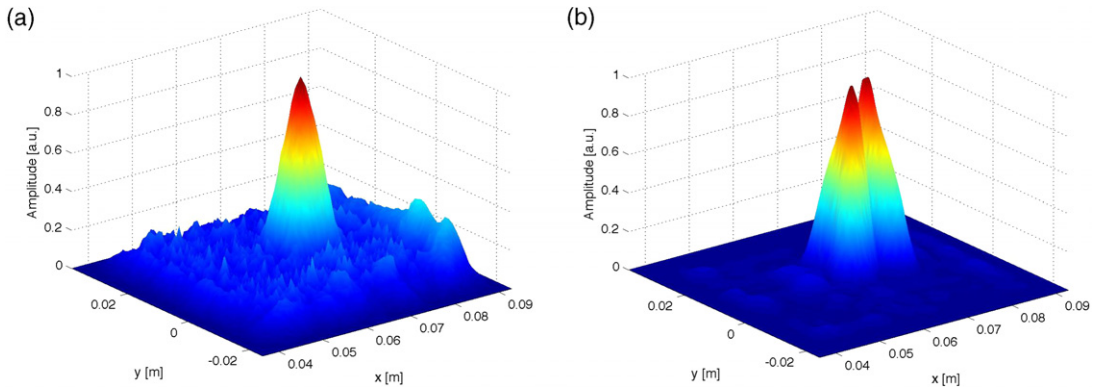

Figure 7. Normalized RMS velocity field (absolute value) over the stubbed region including the defect: (a) harmonic input at 35 kHz excites the first mode of the defect; (b) harmonic input at 63 kHz excites the second mode of the defect.

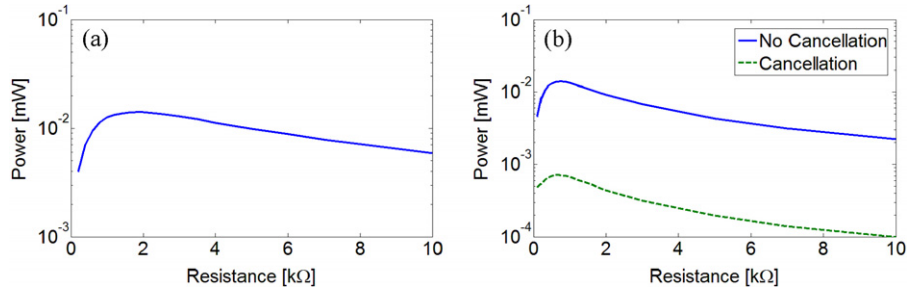

Figure 8. Power output from the defect case at (a) the first resonance of 35 kHz and (b) the second resonance of 63 kHz. The second mode of the defect results in cancellation of the electrical output, which is recovered by using segmented electrodes and proper wiring.

vibration modes of the small defect plate (which can be considered as a Mindlin plate with clamped boundaries as a first approximation [36]).

The MEH concept given in this section represents a perfect elastic analog of the sonic crystal-based acoustic metamaterials configuration proposed in [13], with the advantage that the design considered herein can be envisioned to be transitioned for practical application through tailored design of a foam with periodic inclusions or of a structural substrate with an imperfect array of holes. Moreover, this tuned configuration is suitable for use with conventional tuned (or resonant) energy harvesters [5–8] since the excitation to the harvester takes place at a known frequency.

3.3. Energy harvesting performance

Further experiments are conducted for the defect configuration by placing a 7 mm × 8 mm × 0.2 mm piezoelectric energy harvester plate (STEMiNC Corp.) at the center of the defect. This disk was sliced in half in order to harvest energy from both the first and second mode without charge cancellation [5]. If a single patch were placed over the full sinusoid seen in figure 7(b), one half would be in tension while the other is in compression resulting in cancellation of charge accumulation on the electrodes. As a result, alternative wiring configurations allowed the same segmented piezoelectric plate to harvest power without cancellation at each mode. The piezoelectric plate segments are combined in parallel in both cases. The top and bottom electrodes are all wired together to harvest from the first mode, while the top electrode of one half was wired to the bottom of the other and vice versa in order to harvest from the second mode. Results of these experiments can be seen in figure 8, where over an order of magnitude drop in power occurs due to charge cancellation. This concept is also compatible for use with cantilevered resonant energy harvesters to be located in the defect for base excitation [5] due to the out-of-plane vibrations within the defect.

4. Wave guiding using an acoustic funnel

4.1. Concept of wave channeling and experimental setup

The last concept presented features a metamaterial-inspired array of acoustic scatterers arranged to form an *acoustic funnel* that is hosted on an aluminum plate. This structure is designed with the goal to channel and focus the propagating waves. The operating principle relies on the capability of such a periodic arrangement to manifest bandgaps, based on the periodic spacing of the aluminum stubs. This particular configuration has two complete frequency bandgaps in the ranges 30–60 kHz and 90–130 kHz. Waves at these frequencies do not propagate through the stubbed portion of the plate and are bounded in the region without the slab. Such region is shaped to capture circular crested waves generated by a piezoelectric source, acting as a point source. For excitation within a bandgap (100 kHz), the stubbed array behaves as an almost perfect mirror, reflecting incident waves, and confining their propagation within the desired

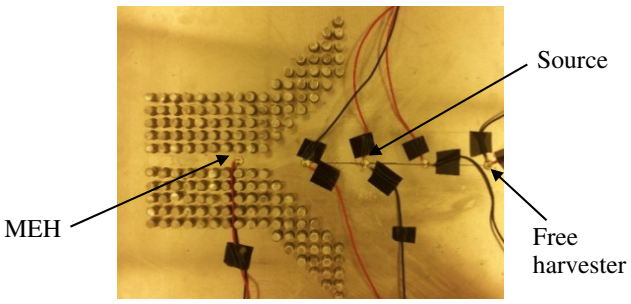

Figure 9. Acoustic funnel formed by the periodic arrangement of stubs featuring an open channel along which waves are guided.

region. The resulting design is pictured in figure 9. As a first relevant result, the full wave propagation field snapshots of figures 10(a)–(c) reveal that this lattice configuration effectively impedes the wave from propagating into the stubbed region. From the snapshots it can also be seen that the wave generated by the source is forced to enter the funnel and travel within the designated channel, and eventually demonstrates the effectiveness of the concept.

4.2. Energy harvesting performance

To evaluate the funnel effectiveness, a free harvester condition (outside the funnel) is taken as a reference, in order to show enhanced energy harvesting performance of the design. Using identical actuation conditions, output voltage data can then be collected from the two aforementioned harvester configurations (namely the one inside the funnel, and the free one). The PZT disk acting as the harvester is then connected to a resistive load, and the voltage across it is recorded as a function of time. Calculating the average power dissipated across the resistor (which is the AC power produced by the piezoelectric energy harvester disk) and plotting it against the resistance yield the results shown in figure 11(a). As can be seen from the graph, there exists an optimal electrical load of maximum power output, which is the same for the two harvesters. There is an average increase of 84.5% in power harvested over the case of a harvester located at the same distance from the source in a region with no lattice. The peak power jumps from 67 μW to 130 μW, showing the effectiveness of this MEH configuration.

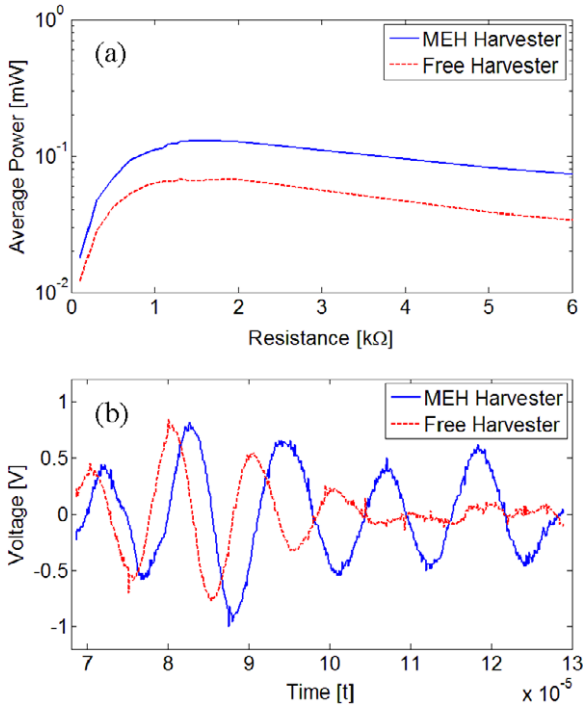

Figure 11. (a) Comparison of power generation performance for MEH and free harvester configurations; (b) voltage across the resistive load of 1.3 kΩ exhibiting the funneling effect in the MEH time history.

Figure 11(b) shows the voltage across a resistive load of 1.3 kΩ for the MEH and free harvester configurations, as recorded during the experimental tests. The funnel effect is clearly visible, as the free harvester collects voltage data nearly identical in form (not amplitude) to the input signal whereas the MEH harvester has an extended time signature that is the result of vibrations reflecting off the funnel and proceeding into the channel.

5. Conclusions

This paper presented structure-borne wave energy harvesting concepts by exploiting metamaterial-based and metamaterial-inspired electroelastic systems for performance enhancement in piezoelectric power generation. The metamaterial energy harvester (MEH) systems introduced herein transform the

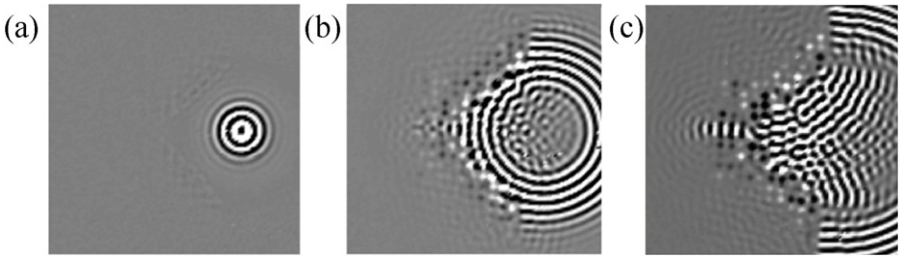

Figure 10. (a)–(c) Snapshots of the wavefield recorded for burst excitation at 100 kHz at successive instants of time show the wave confinement operated by the funnel.

incoming structure-borne wave energy into electrical energy by coupling the metamaterial and electroelastic domains. Three concepts were proposed for *broadband* and *tuned* wave energy harvesting: (1) wave focusing using a metamaterial-inspired parabolic acoustic mirror (for broadband energy harvesting), (2) energy localization using an imperfection in a 2D lattice structure (for tuned energy harvesting), and (3) wave guiding using an acoustic funnel (for narrow-to-broadband energy harvesting). Experiments were conducted for performance comparison of the MEH systems with free harvesters and dramatic performance improvement is verified for the acoustic mirror and funnel arrangements. These mirror and funnel concepts can be combined with broadband energy harvesters while the imperfection concept is well suited for tuned (or resonant) energy harvesters covered in the literature of vibration-based energy harvesting. The MEH concepts introduced herein can enable potential system-level applications such as low-power electricity generation for structural monitoring sensor networks and acoustic energy harvesting while absorbing undesired noise. Moreover, the high frequencies involved in MEH systems may open new avenues for the implementation of MEMS energy harvesters.

References

[1] Magoteaux K C, Sanders B and Sodano H A 2008 Investigation of an energy harvesting small unmanned air vehicle *Proc. SPIE* **6928** 692823

[2] Anton S R, Erturk A and Inman D J 2012 Multifunctional unmanned aerial vehicle wing spar for low-power generation and storage *J. Aircr.* **49** 292–301

[3] Erturk A 2011 Piezoelectric energy harvesting for civil infrastructure system applications: moving loads and surface strain fluctuations *J. Intell. Mater. Syst. Struct.* **22** 1959–73

[4] Ali S F, Friswell M I and Adhikari S 2011 Analysis of energy harvesters for highway bridges *J. Intell. Mater. Syst. Struct.* **22** 1929–38

[5] Erturk A and Inman D J 2011 *Piezoelectric Energy Harvesting* (Chichester: Wiley)

[6] Roundy S and Wright P K 2004 A piezoelectric vibration based generator for wireless electronics *Smart Mater. Struct.* **13** 1131–42

[7] duToit N E and Wardle B L 2006 Performance of microfabricated piezoelectric vibration energy harvesters *Integr. Ferroelectr.* **83** 13–32

[8] Erturk A and Inman D J 2009 An experimentally validated bimorph cantilever model for piezoelectric energy harvesting from base excitations *Smart Mater. Struct.* **18** 025009

[9] Rupp C J *et al* 2009 Design of piezoelectric energy harvesting systems: a topology optimization approach based on multilayer plates and shells *J. Intell. Mater. Syst. Struct.* **20** 1923–39

[10] Cook-Chennault K A, Thambi N and Sastry A M 2008 Powering MEMS portable devices—a review of non-regenerative and regenerative power supply systems with special emphasis on piezoelectric energy harvesting systems *Smart Mater. Struct.* **17** 043001

[11] Kim S H *et al* 2009 An electromagnetic energy scavenger from direct airflow *J. Micromech. Microeng.* **19** 094010

[12] Horowitz S B *et al* 2006 A MEMS acoustic energy harvester *J. Micromech. Microeng.* **16** S174–81

[13] Wu L Y, Chen L W and Liu C M 2009 Acoustic energy harvesting using resonant cavity of a sonic crystal *Appl. Phys. Lett.* **95** 013506

[14] Wang W C *et al* 2010 Acoustic energy harvesting by piezoelectric curved beams in the cavity of a sonic crystal *Smart Mater. Struct.* **19** 045016

[15] Rupp C J, Dunn M L and Maute K 2010 Switchable phononic wave filtering, guiding, harvesting, and actuating in polarization-patterned piezoelectric solids *Appl. Phys. Lett.* **96** 111902

[16] Allen J J and Smits A J 2001 Energy harvesting eel *J. Fluids Struct.* **15** 629–40

[17] Pobering S, Ebermeyer S and Schwesinger N 2009 Generation of electrical energy using short piezoelectric cantilevers in flowing media *Proc. SPIE* **7288** 728807

[18] Tang L S, Paidoussis M P and Jiang J 2009 Cantilevered flexible plates in axial flow: energy transfer and the concept of flutter-mill *J. Sound Vib.* **326** 263–76

[19] Erturk A *et al* 2010 On the energy harvesting potential of piezoaeroelastic systems *Appl. Phys. Lett.* **96** 184103

[20] De Marqui C, Erturk A and Inman D J 2010 Piezoaeroelastic modeling and analysis of a generator wing with continuous and segmented electrodes *J. Intell. Mater. Syst. Struct.* **21** 983–93

[21] Akaydin H D, Elvin N and Andreopoulos Y 2010 Wake of a cylinder: a paradigm for energy harvesting with piezoelectric materials *Exp. Fluids* **49** 291–304

[22] Sousa V C *et al* 2011 Enhanced aeroelastic energy harvesting by exploiting combined nonlinearities: theory and experiment *Smart Mater. Struct.* **20** 094007

[23] Bryant M and Garcia E 2011 Modeling and testing of a novel aeroelastic flutter energy harvester *J. Vib. Acoust.—Trans. ASME* **133** 011010

[24] Dunnmon J A *et al* 2011 Power extraction from aeroelastic limit cycle oscillations *J. Fluids Struct.* **27** 1182–98

[25] Kwon S D 2010 A *T*-shaped piezoelectric cantilever for fluid energy harvesting *Appl. Phys. Lett.* **97** 164102

[26] St. Clair D *et al* 2010 A scalable concept for micropower generation using flow-induced self-excited oscillations *Appl. Phys. Lett.* **96** 144104

[27] Ruzzene M and Scarpa F 2005 Directional and band-gap behavior of periodic auxetic lattices *Phys. Status Solidi* b **242** 665–80

[28] Ruzzene M, Scarpa F and Soranna F 2003 Wave beaming effects in two-dimensional cellular structures *Smart Mater. Struct.* **12** 363–72

[29] Movchan A B, Movchan N V and Haq S 2006 Localised vibration modes and stop bands for continuous and discrete periodic structures *Mater. Sci. Eng.* A **431** 175–83

[30] Torrent D and Sánchez-Dehesa J 2007 Acoustic metamaterials for new two-dimensional sonic devices *New J. Phys.* **9** 323

[31] Psarobas I, Stefanou N and Modinos A 2000 Scattering of elastic waves by periodic arrays of spherical bodies *Phys. Rev.* B **62** 278–91

[32] Deymier P A *et al* 2008 Focusing of acoustic waves by flat lenses made from negatively refracting two-dimensional phononic crystals *Rev. Mex. Fis.* **54** 74–81

[33] Carrara M *et al* 2012 Dramatic enhancement of structure-borne wave energy harvesting using an elliptical acoustic mirror *Appl. Phys. Lett.* **100** 204105

[34] Senesi M, Xu B L and Ruzzene M 2010 Experimental characterization of periodic frequency-steerable arrays for structural health monitoring *Smart Mater. Struct.* **19** 055026

[35] Baravelli E *et al* 2011 Double-channel, frequency-steered acoustic transducer with 2D imaging capabilities *IEEE Trans. Ultrason. Ferroelectr. Freq. Control* **58** 1430–41

[36] Dawe D and Roufaeil O 1980 Rayleigh–Ritz vibration analysis of Mindlin plates *J. Sound Vib.* **69** 345–59